Thermochimica Acta 499 (2010) 65–70

Contents lists available at ScienceDirect

Thermochimica Acta

journal homepage: www.elsevier.com/locate/tca

Enthalpy of formation of the La–Mg intermediate phases

A. Berche[a], F. Marinelli[b], J. Rogez[a,*], M.-C. Record[a]

[a] CNRS, IM2NP (UMR 6242), Aix-Marseille Université, FST Saint-Jérôme, Av. Escadrille Normandie Niémen, Case 251, F-13397 Marseille Cedex, France
[b] Physique des Interactions Ioniques et Moléculaires (UMR 6633), Aix-Marseille Université, FST Saint Jérôme, Av. Escadrille Normandie Niémen, Case 242, F-13397 Marseille Cedex, France

ARTICLE INFO

Article history:
Received 4 September 2009
Received in revised form 3 November 2009
Accepted 9 November 2009
Available online 17 November 2009

Keywords:
Enthalpy of formation
Drop-calorimetry
Density functional theory
Lanthanum
Magnesium

ABSTRACT

The aim of this work is to complete the available set of thermodynamic data on the La–Mg system in order to get reliable optimisation of this system by the CALPHAD method. Indeed the CALPHAD method requires a large set of consistent input data including both phase diagram and thermodynamic data.

The enthalpies of formation of the La–Mg intermediate compounds were determined at 298 K by means of solution calorimetry in liquid Sn in a Tian–Calvet calorimeter. In these experiments, the partial enthalpies of solution of the compounds at infinite dilution in liquid tin were measured at 665 K.

The enthalpies of formation of LaMg, $LaMg_2$ and La_2Mg_{17} compounds were also calculated at 0 K by density functional theory to compare experimental and calculated values.

1. Introduction

The La–Mg–Zn alloys are very attractive for the transport industry since they have a light weight though with a high specific strength [20,21,26]. The optimisation of these alloys needs knowledge on the phase diagram of the La–Mg–Zn system, and consequently on the phase diagram of its constitutive systems, e.g. La–Mg.

Currently, determination of phase diagram can be achieved by numerical calculations. These calculations need experimental thermodynamic quantities, such as activities of the elements, enthalpies of mixing in the liquid phase or enthalpies of formation of the solid intermediate phases as input data.

The aim of this work is therefore to provide enthalpy of formation of the La–Mg compounds for future calculations.

2. Literature data

The La–Mg phase diagram retained by Massalski [16] corresponds to the assessment of the La–Mg phase diagram performed in 1988 by Nayeb-Hashemi and Clark [13]. This phase diagram contains five intermediate phases: LaMg, $LaMg_2$, $LaMg_3$, La_2Mg_{17} and $LaMg_{12}$. $LaMg_2$ only exists at high temperatures, between 725 and 775 °C; the other phases exist from room temperature up to their melting points.

However, the Mg-rich region was subsequently reinvestigated in 1995 by Giovannini et al. [19] and the existence of an additional intermediate phase La_5Mg_{41} has been established.

Recently, based on a critical review of the La–Mg phase diagram and additional experimental investigations, Berche et al. [29] suggested a new phase diagram in which the discrepancies encountered in literature are clarified. The existence of La_5Mg_{41} and its stability range were confirmed. The metastability of the $LaMg_2$ phase at low temperatures was ascertained. All the invariant reactions of this phase diagram were clearly defined and assigned, in particular the melting temperatures of La_5Mg_{41} and La_2Mg_{17}.

Therefore six intermediate compounds (LaMg, $LaMg_2$, $LaMg_3$, La_2Mg_{17}, $LaMg_{12}$, and La_5Mg_{41}) exist in the La–Mg phase diagram, whereas two of them ($LaMg_2$ and La_5Mg_{41}) are not stable at room temperature.

The enthalpy of mixing of liquid La–Mg alloys was determined by Agarwal et al. [18] between 970 and 1060 K. Two different methods were used: (1) direct enthalpy measurements by starting from the pure metals and (2) determination of the integral enthalpy from partial solution enthalpy measurements of the elements in an alloy. The extrapolated maximum of the enthalpy of mixing is about $-13\ kJ\ mol^{-1}$ at about 23.0 at.% La which corresponds to the composition of the compound ($LaMg_3$) bearing the highest melting temperature.

Vapour pressure measurements over La–Mg liquid alloys between 950 and 1133 K were reported by Afanas'ev et al. [7]. The results were used to calculate the activity of La and Mg, their Gibbs energy, and their enthalpy and entropy of mixing. The negative maximum of the concentration dependence of Gibbs

* Corresponding author. Tel.: +33 04 91 28 28 87; fax: +33 04 91 28 28 86.
E-mail address: j.rogez@univ-cezanne.fr (J. Rogez).

0040-6031/$ – see front matter © 2009 Elsevier B.V. All rights reserved.
doi:10.1016/j.tca.2009.11.003

Table 1
Partial enthalpies of solution at infinite dilution in tin bath at 665 K and enthalpies of formation of the La–Mg intermediate phases (kJ/mol atom).

Phase	$\Delta_{Sol}\bar{H}^{\infty}$ (kJ/mol of atom)	$\Delta_f H$ (kJ/mol of atom)					
		Acidic calorimetry (298 K) [1]	Acidic calorimetry (298 K) [15]	CALPHAD (298 K) [27]	DFT (0 K) [30]	Metallic calorimetry (298 K) (this work)	DFT (0 K) (this work)
La	−263.0 ± 7.0	–	–	–	–	–	–
Mg	−13.3 ± 0.7	–	–	–	–	–	–
LaMg	−126.0 ± 1.6	−11.9	−7.1	−16.7	−11.3	−12.1 ± 3.4	−11.25
$LaMg_2$	−80.7 ± 2.0	–	−2.4	−8.9	−12.2	−15.8 ± 3.5	–
$LaMg_3$	−60.0 ± 1.0	−13.5	−27.7	−19.7	−13.3	−15.7 ± 2.4	−17.27
La_2Mg_{17}	−31.8 ± 0.5	–	−0.7	−8.7	−7.7	−7.8 ± 1.7	−7.84
$LaMg_{12}$	−27.6 ± 1.7	–	–	−6.4	−6.0	−4.9 ± 1.7	–

Table 2
Compositions and annealing conditions of the samples and XRD and SEM results.

Alloys	Comp. at.% Mg	Annealing conditions		Phases		Space group	Cell parameters (Å)	
		T (K)	Duration (h)	SEM	XRD		This work	Literature
LaMg	50.0	850	100	LaMg	LaMg	$Pm-3m$	a = 3.97	a = 3.96 [2]
$LaMg_2$	66.7	1029	100	$LaMg_2$	$LaMg_2$	$Fd-3m$	a = 8.79	a = 8.79 [3] a = 8.81 [28]
$LaMg_3$	75.0	840	100	$LaMg_3$	$LaMg_3$	$Fm-3m$	a = 7.48	a = 7.45–7.47 [2]
La_2Mg_{17}	89.5	840	213	–	La_2Mg_{17}	$P6_3/mmc$	a = 10.37 c = 10.22	a = 10.365 c = 10.244 [5]
$LaMg_{12}$	92.1	860	70	–	$LaMg_{12}$	$I4/mmm$	–	a = 10.32–10.37 b = 10.32–10.37 c = 77.24–77.56 [19]

energy coincided with the composition of the congruently melting compound $LaMg_3$.

The shift of the negative maximum entropy and enthalpy to the Mg side suggest short-range ordering in these liquid alloys.

The vapour pressure of Mg over La–Mg binary alloys with compositions 20 and 21 at.% Mg were measured by the Knudsen effusion method from 660 to 910 K in Ref. [6]. From these measurements the authors evaluated the standard free energy of formation of LaMg.

The enthalpies of formation of LaMg and $LaMg_3$ at 298 K were first measured by Canneri [1]. They used solution calorimetry in hydrochloric acid 8.8N. Later on, Piagai et al. [15] performed the same kind of measurements on LaMg and $LaMg_3$ and extended them to $LaMg_2$ and La_2Mg_{17} by using hydrochloric acid 1N as dissolution bath.

In 2004, Guo et al. performed a critical assessment of the La–Mg system by using the CALPHAD method [27]. However, they only considered five intermediate phases: LaMg, $LaMg_2$, La_2Mg_{17}, $LaMg_3$ and $LaMg_{12}$. Among other thermodynamic data, this assessment provides calculated values for the enthalpy of formation of each intermediate phase. The initial values used for this assessment by the author were calculated using the Miedema model.

Recently, Wang et al. [30] calculated the enthalpy of formation of the intermetallic phases of this system at 0 K by using density functional theory. These calculations were performed using Vienna ab initio Simulation Package (VASP) with projector augmented plane-wave pseudopotential (PAW) and generalized gradient approximation (GGA). The energy of cutoff of atomic wave functions was set at 300 eV.

All the values available in literature for the enthalpy of formation at 298 K of the La–Mg intermediate phases are reported in Table 1.

Large discrepancies between these values can be observed. This statement holds true when comparing experimental data, although they were determined with the same method. This behaviour is not surprising since in the acidic dissolution method the accuracy is very low. In fact, the final states of dissolution are often poorly defined as the dissolved elements present several oxidation states. Moreover, the dissolution enthalpy of the pure elements (Mg and hcp-La) in acids is very large in comparison with the calculated enthalpy of formation of the compounds; a ratio of 100 is quite usual.

This review clearly shows that no reliable data for the enthalpy of formation of the La–Mg intermediate phases is available in literature so far. The aim of the present work is to determine these quantities in order to fill in this gap.

3. Experimental and calculation procedure

3.1. Sample preparation

The alloys were prepared from a mixture of pure constitutive elements La and Mg, weighed in the stoichiometric ratio.

The characteristics of these elements are as follows: La ingot (99.9%+, Huhhot Jinrui Rare Earth Co. LTD.) and Mg shots (99.98%, Aldrich). Both magnesium and lanthanum were handled in a glove box (<1 ppm O_2, <20 ppm H_2O) to protect them from oxidation.

Weighed amounts of the pure elements were placed into tantalum crucibles (18 mm in diameter and 11 mm of height). These crucibles were cold-stamped from a tantalum sheet, with a thickness of 0.25 mm, supplied by Technicome. They were filled and sealed by a tungsten inert gas (TIG) welding, under argon atmosphere in a glove box.

Samples were then heated up to 1250 K for 10 min. This treatment, which aimed to rapidly get a homogeneous alloy, was followed by an annealing treatment to reach the equilibrium state. The annealing conditions are detailed in Table 2.

3.2. Sample characterization

The phase identification of the samples was performed by X-ray diffraction and scanning electron microprobe.

The diffraction patterns were recorded on a Philips Expert diffractometer (with a copper $K_{\alpha 1}$ anticathode) in the [10–100°] 2θ range, with a step size of 0.01671° and a step time of 130 s. The lattice parameters were determined from these diffraction patterns using the PowderCell program [25].

SEM measurements were performed on a FEG XL30S—Oxford Instruments. This scanning electron microscope is equipped with an energy dispersive X-ray spectroscope which allows quantitative analysis of the phases.

3.3. Calorimetric measurements

The solution calorimetric measurements were carried out in a home-made Tian–Calvet calorimeter extensively described in literature [4,9]. Each of the twin cells is surrounded by a thermopile with more than 200 thermocouples. The calorimeter is suitable for temperatures up to 1200 K and heated by a resistance furnace.

Pieces of Sn (solvent) with a total mass of about 2 g were placed into a graphite crucible (12 mm in diameter, 70 mm in height) which was put inside the quartz tube, itself introduced in one of the calorimeter cells. Before starting the experiment, the quartz tube was flushed several times with high purity argon. Finally, during the experiments, the sample was subjected to an argon flow of 10 ml/min. Small pieces (10–30 mg) of samples were dropped from room temperature into the liquid Sn bath maintained at 665 K. At the end of each set of measurements, the calorimeter was calibrated by three additions of 20, 40 and 100 mg of standard α-Al_2O_3 supplied by NIST (National Institute of Standards and Technology, Gaithersburg, MD, USA).

3.4. DFT calculations

The enthalpy of formation of the La–Mg compounds were calculated using density functional theory (DFT) with the Perdew–Wang functional [12] of the generalized gradient approximation (GGA) as implemented in the QUANTUM-ESPRESSO PWscf ab initio package [33].

Sampling of the irreducible Brillouin zone was performed with $[6 \times 6 \times 6]$ and $[8 \times 8 \times 8]$ regular Monkhorst-Pack grids [8] (i.e. 40 and 70 k-points, respectively). These two grids were used in order to check the convergence of the calculation. Ultrasoft pseudopotentials of Vanderbilt [17] with non linear core correction were used for both La and Mg. The kinetic energy cutoff was 25 Ry. The smearing method with a Methfessel and Paxton broadening function [14] fixed at 0.02 Ry was applied as reported by Turner et al. [23].

For lanthanum, the (5s), (5p), (5d), (6s) and (6p) atomic orbitals were treated as valence levels corresponding to a reference configuration $(5s)^2, (5p)^6, (5d), (6s)^{3/2}$ and $(6p)^{1/2}$ by GGA spin unrestricted calculations.

For both lanthanum and magnesium, the cohesive energies (E_c) were calculated by using the experimental crystal parameters. These energies are given with respect to the energies of the spin polarized atoms for La and Mg in their ground state.

Table 4
Distortion matrix for La in Å.

Atom La	Δx coordinate	Δy coordinate	Δz coordinate
1	0.1079	0.0544	−0.0427
2	0.1207	0.0539	−0.0211
3	−0.1076	−0.0401	−0.0100
4	−0.1209	−0.0682	0.0738

The energies of formation were calculated using the following formula:

$$\Delta E_f = \frac{E(La_nMg_m) - n\,E(La) - m\,E(Mg)}{n+m} \quad (1)$$

where $E(La_nMg_m)$ is the total energy of La_nMg_m, n and m being the number of La and Mg atoms in the unit cell, E(La) and E(Mg) the optimized bulk energies of hcp-La and hcp-Mg, respectively. These total energies were determined using the experimental crystal parameters.

4. Results and discussion

4.1. Phase identification

Results obtained by SEM and XRD are gathered in Table 2. All the samples were single phased within the error margin of the observations. PowderCell program [25] was used to analyse the XRD patterns. From the crystal structure of a phase, PowderCell calculates the theoretical pattern and by using a refinement algorithm, the program determines the lattice parameter(s) corresponding to the experimental diffraction pattern. The lattice parameters obtained for each phase are compared to those reported in literature. The agreement is good; the maximum observed deviation is lower than 0.35%.

4.2. Preliminary DFT calculations

Preliminary DFT calculations were performed to test the validity of our method.

The calculated cohesive energies (in eV/at.) of La and Mg are given in Table 3. They are compared with calculated and experimental values previously reported in literature.

Regarding the magnesium, our result is in full agreement with that obtained by Pozzo et al. [31] using Perdew–Wang [12] functional.

For the lanthanum, the cohesive energy obtained in the present work is the closest calculated value to the experimental one. According to Delin et al. [24], both local density approximation (LDA) and generalized gradient approximation (GGA) using Perdew–Wang functional overestimate the cohesive energy E_c of La. This assertion agrees with our result.

The effect of a change of the internal positions on the total energy was tested in lanthanum by considering small displacements of the atoms from their symmetrical positions. The hcp-La contains 4

Table 3
Cohesive energies for La and Mg in eV/at.

Element	Values from this work	Other theoretical values				Experimental values
	DFT GGA (PW86)	DFT LDA (HL)	DFT GGA (PBE)	DFT GGA (PW91)	Quantum Monte-Carlo (DMC)	
La	4.651	5.49[a]	4.23[b]	4.78[a]		4.467[c]
Mg	1.45	1.74[d]	1.47[d]	1.45[d]	1.51[d]	1.51[e]

[a] Ref. [24].
[b] Ref. [32].
[c] Ref. [11].
[d] Ref. [31].
[e] Ref. [22].

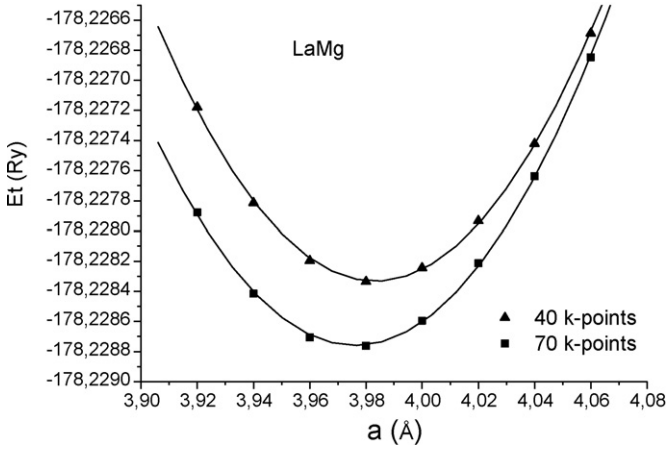

Fig. 1. Calculated total energy E_t of the LaMg compound versus lattice parameter for two sets of k-points.

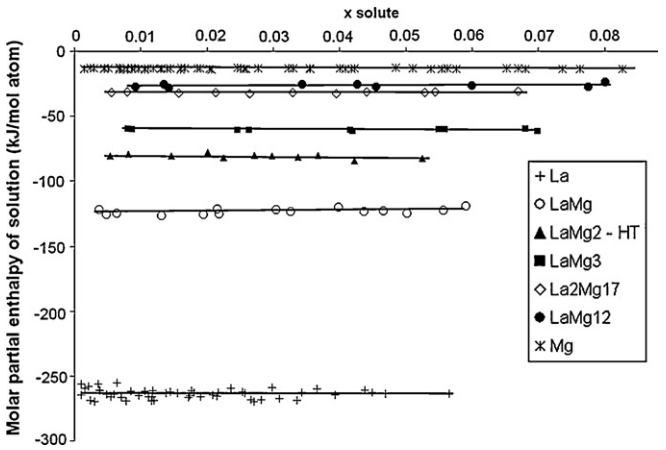

Fig. 3. Molar partial enthalpies of solution in liquid Sn at 665 K of solid La, Mg and La–Mg intermediate phases.

atoms per unit cell. The distortion matrix of the atomic positions (in Å) is given in Table 4.

The variation of the total energy is relatively small and amounts only to 0.06 Ry.

The total energy of LaMg was calculated using various lattice parameters. Two sets of k-points, namely 40 and 70, were used to check the convergence of the calculations. The corresponding evolutions are depicted in Fig. 1. Quadratic fits of these data lead to the same lattice parameter $a = 3.98$ Å within 0.007 Å of deviation.

We can notice a good agreement with the experimental values $a = 3.96$ Å [2] and $a = 3.97$ Å [present work] (see Table 2).

Similar calculations were performed on $LaMg_3$. The evolution of the total energy versus lattice parameter is depicted in Fig. 2. The lattice parameter $a = 7.52$ Å of $LaMg_3$ was determined from the fit of the curve. Although the deviation from the experimental data ($a = 7.45$–7.47 Å [2] and $a = 7.48$ Å [present work]) is larger than in the case of the LaMg compound, the calculated result is still satisfactory.

4.3. Enthalpies of formation of the solid phases

The enthalpy of formation was determined experimentally at 298 K for LaMg, $LaMg_2$, $LaMg_3$, La_2Mg_{17} and, $LaMg_{12}$. DFT calculations were performed at 0 K for LaMg, $LaMg_3$ and La_2Mg_{17}.

The molar partial enthalpies of solution of La, Mg and the intermediate phases in liquid tin were determined by successive additions of small pieces of material into the tin bath at 665 K. All the obtained values are gathered in the appendix and plotted versus the molar fraction of the added material in Fig. 3.

In the investigated composition range, the heat of solution is approximately a linear function of the composition, x_{solute}. Therefore the $\Delta_{Sol}\bar{H}$ values were fitted to a polynomial of first order and extrapolated to infinite dilution ($x_{Sn} = 1$) in order to obtain $\Delta_{Sol}\bar{H}^{\infty}$. The partial enthalpies of solution at infinite dilution for La, Mg and the La–Mg intermediate phases referred to liquid tin at 665 K and to solid elements or compounds in their crystalline structure at 298 K are given in Table 1. The large exothermic effect observed with La indicates a strong interaction between Sn and La. This is consistent with the known existence of stable compounds between La and Sn in the solid state and can be attributed to the fairly large electronegativity difference between the components [10].

The enthalpies of formation, $\Delta_f H^{298}$ of the La–Mg compounds were obtained from the difference between the heats of solution at infinite dilution of the pure components and those of the compounds following the formula:

$$\Delta_f H^{298}(A_xB_y) = x\,\Delta_{Sol}\bar{H}^{\infty}(A) + y\,\Delta_{Sol}\bar{H}^{\infty}(B) - \Delta_{Sol}\bar{H}^{\infty}(A_xB_y) \quad (2)$$

The obtained values are gathered in Table 1. They are compared to those calculated at 0 K by DFT. We can notice a good agreement between them. DFT values lie in the uncertainty range of calorimetric measurements.

Our results, both experimental (at 298 K) and calculated (at 0 K) are compared to the literature data (at 298 K or at 0 K) in Fig. 4.

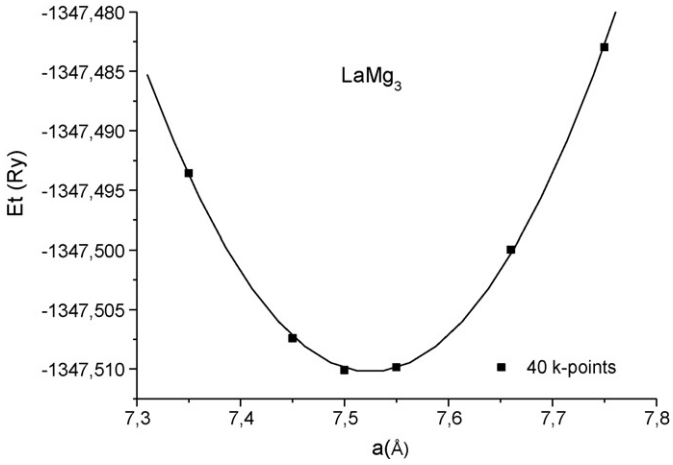

Fig. 2. Calculated total energy E_t of the $LaMg_3$ compound versus lattice parameter.

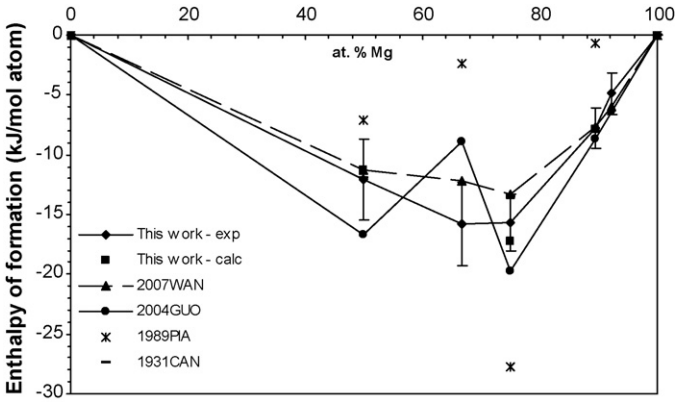

Fig. 4. Enthalpies of formation of La–Mg solid phases determined at 0 K by DFT and at 298 K by solution calorimetry, compared to the literature data.

The enthalpies of formation, determined by Canneri et al. [1] for LaMg and $LaMg_3$, and by Wang et al. [30] for both phases lie within the uncertainty range of our results. The evolution of the enthalpy of formation of the phases with the composition of the phases determined in this work is consistent with those of Wang et al. especially concerning $LaMg_2$.

However, the values reported by Piagai et al. [15] are very far from those reported by other authors. This could be due to the low purity (95%) of the magnesium used [15]. However, the large scattering of these values could also suggest a non-equilibrium state for the studied alloys.

The optimized values reported by Guo et al. [27] for LaMg, $LaMg_2$ and $LaMg_3$ differ substantially from both experimental and calculated values. Especially, it had been shown that the instability of $LaMg_2$ at low temperature is not directly linked to a lower enthalpy of formation. A new assessment of this system using the new set of value described here will be soon published.

5. Conclusion

A new set of enthalpies of formation were determined in this work for the La–Mg intermediate phases. Both experimental measurements and calculations were performed.

Measurements were carried out by means of solution calorimetry in liquid Sn in a Tian–Calvet calorimeter. The partial enthalpies of solution of the phases at infinite dilution were measured at 665 K in liquid tin and the enthalpies of formation were calculated at 298 K.

Calculations were performed using the generalized gradient approximation density functional theory (GGA-DFT) with the Perdew–Wang 86 functional. The enthalpies of formation were calculated at 0 K.

Since this set of values seems to be consistent, this work may help in a more reliable assessment of the La–Mg system.

Appendix A.

Molar partial solution enthalpies (in kJ/mol of atom) obtained at 665 K for La, Mg and the La–Mg intermediate phases in pure liquid Sn.

X	$\overline{\Delta H_m}$	$\Delta(\overline{\Delta H_m})$
Lanthane		
0.0021	−257.9	6.65
0.0117	−266.0	1.82
0.0176	−261.1	0.36
0.0236	−259.5	1.42
0.0298	−259.2	0.32
0.0366	−259.7	0.31
0.0439	−260.6	0.34
0.0106	−261.8	0.34
0.0180	−262.8	0.28
0.0257	−263.0	0.25
0.0343	−262.5	0.36
0.0450	−262.8	0.29
0.0566	−263.4	0.18
0.0048	−264.2	0.38
0.0118	−261.5	0.97
0.0190	−266.1	1.80
0.0282	−268.3	0.39
0.0335	−268.5	1.47
0.0394	−264.8	0.44
0.0469	−263.5	0.57
0.0038	−261.1	0.47
0.0071	−266.5	0.62
0.0097	−265.2	2.34
0.0010	−264.6	4.22
0.0055	−265.9	1.26
0.0112	−265.8	1.52

Appendix A (*Continued*)

X	$\overline{\Delta H_m}$	$\Delta(\overline{\Delta H_m})$
0.0030	−269.9	0.32
0.0085	−262.0	0.47
0.0120	−268.9	0.90
0.0156	−263.0	0.40
0.0209	−264.4	2.00
0.0253	−262.0	6.44
0.0038	−260.9	0.29
0.0138	−263.2	1.51
0.0174	−264.9	1.03
0.0217	−262.7	0.35
0.0266	−268.3	2.04
0.0024	−268.7	0.50
0.0078	−269.3	0.57
0.0145	−262.2	0.39
0.0215	−265.5	0.34
0.0271	−269.9	0.47
0.0309	−267.4	2.07
0.0016	−259.5	7.05
0.0059	−264.0	0.56
0.0116	−269.0	0.47
0.0172	−266.5	1.73
Magnesium		
0.0024	−12.5	0.41
0.0068	−12.8	0.48
0.0086	−12.8	0.59
0.0110	−12.9	0.24
0.0144	−13.0	0.35
0.0189	−13.0	0.20
0.0045	−13.2	0.53
0.0075	−13.5	0.19
0.0106	−13.9	0.15
0.0161	−12.7	0.04
0.0015	−13.4	0.54
0.0030	−13.3	0.26
0.0070	−12.9	0.92
0.0097	−13.4	0.25
0.0130	−13.7	0.09
0.0167	−13.2	0.50
0.0068	−14.0	0.12
0.0207	−13.9	0.44
0.0356	−13.6	0.08
0.0511	−13.2	0.64
0.0681	−13.7	1.11
0.0826	−13.7	0.25
0.0045	−13.7	0.35
0.0080	−13.8	0.40
0.0119	−13.2	0.12
0.0161	−13.8	0.22
0.0204	−13.6	0.21
0.0256	−13.4	0.41
0.0051	−12.9	0.12
0.0091	−13.0	0.11
0.0132	−13.2	0.19
0.0185	−12.9	0.30
0.0251	−13.3	0.41
0.0323	−12.9	0.47
0.0401	−13.2	0.14
0.0140	−13.4	0.18
0.0330	−13.0	0.14
0.0554	−13.6	0.13
0.0669	−13.1	0.21
0.0763	−13.6	0.44
0.0107	−13.5	0.12
0.0259	−13.5	−0.16
0.0409	−13.5	−0.22
0.0576	−13.7	−0.31
0.0087	−13.3	0.13
0.0246	−12.6	0.19
0.0355	−13.3	0.20
0.0423	−13.2	0.26
0.0485	−12.7	0.22
0.0563	−12.9	0.09
0.0097	−13.5	0.17
0.0277	−13.1	0.07
0.0418	−13.4	0.15
0.0538	−13.5	0.18

Appendix A (*Continued*)

X	$\overline{\Delta H_m}$	$\Delta(\overline{\Delta H_m})$
0.0652	−13.0	0.22
0.0737	−13.7	0.41
$LaMg_2$-HT		
0.0054	−80.7	0.51
0.0146	−80.9	0.95
0.0225	−82.1	0.36
0.0298	−80.5	0.42
0.0367	−80.2	0.81
0.0081	−79.2	0.18
0.0202	−77.9	0.67
0.0272	−80.0	0.31
0.0338	−81.6	0.98
0.0423	−84.4	0.14
0.0525	−82.7	0.20
$LaMg_3$		
0.0087	−60.1	0.50
0.0263	−60.5	0.35
0.0419	−61.4	0.67
0.0550	−60.1	1.15
0.0680	−59.7	0.97
0.0080	−59.9	0.26
0.0246	−60.8	0.24
0.0416	−60.6	1.72
0.0559	−60.1	2.33
0.0699	−61.7	0.35
LaMg		
0.0049	−125.9	0.65
0.0132	−127.1	1.04
0.0219	−125.4	0.23
0.0326	−123.8	0.21
0.0467	−123.2	0.15
0.0038	−122.4	0.59
0.0216	−121.9	0.53
0.0437	−123.5	0.61
0.0557	−122.9	0.98
0.0064	−125.0	0.72
0.0195	−126.0	0.84
0.0305	−122.3	0.94
0.0399	−120.5	0.58
0.0502	−124.8	0.36
0.0590	−119.5	0.39
La_2Mg_{17}		
0.0080	−31.2	0.34
0.0213	−31.5	0.20
0.0329	−31.7	0.23
0.0441	−31.4	0.11
0.0544	−31.2	0.07
0.0056	−31.5	0.14
0.0157	−32.1	0.22
0.0265	−32.5	0.16
0.0395	−32.5	0.23
0.0529	−31.9	0.42
0.0669	−31.0	0.09
$LaMg_{12}$		
0.0135	−25.8	0.15
0.0427	−25.7	0.19
0.0093	−27.4	0.19
0.0344	−25.7	0.16
0.0600	−26.6	0.15
0.0801	−24.0	0.20
0.0143	−28.3	0.13
0.0456	−27.5	0.21
0.0776	−27.7	0.33

References

[1] G. Canneri, Metall. Ital. 23 (1931) 803–823.
[2] A. Rossi, Gazz. Chim. Ital. 64 (1934) 774–778.
[3] F. Laves, Naturwissenschaften 31 (1943) 96.
[4] E. Calvet, H. Prat, Recent Progress in Microcalorimetry, Pergamon Press, 1963.
[5] V.I. Evdokimenko, P.I. Kripyakevich, Kristallografiya 8 (2) (1963) 186–193.
[6] J.R. Ogren, N.J. Magnani, J.F. Smith, Trans. Metall. Soc. AIME 239 (6) (1967) 766–771.
[7] Yu.A. Afanas'ev, A.P. Bayanov, Yu.A. Frolov, Izv. An. SSSR Met. 1 (1975) 186–190.
[8] H.J. Monkhorst, J.D. Pack, Phys. Rev. B 13 (1976) 5188–5192.
[9] G. Hohne, Calorimetry: Fundamentals and Practice, Verlag Chemie, 1984.
[10] C. Colinet, A. Pasturel, A. Percheron-Guégan, J.C. Achard, J. Less Common Met. 102 (1984) 167–177.
[11] B. Johanson, P. Munck, J. Less Common Met. 100 (1984) 49–70.
[12] J.P. Perdew, Y. Wang, Phys. Rev. B 33 (1986) 8800–8802.
[13] A.A. Nayeb-Hashemi, J.B. Clark, Bull. Alloy Phase Diagr. 9 (2) (1988) 172–173.
[14] M. Methfessel, A.F. Paxton, Phys. Rev. B 40 (1989) 3616–3621.
[15] I.N. Piagai, A.V. Vakhobov, N.G. Schmidt, O.V. Khikhareva, M.I. Numanov, Dokl. Acad. Nauk. Tadzhikskoi SSR 32 (9) (1989) 605–607.
[16] T.B. Massalski, Binary Alloys Phase Diagrams, 2nd ed., American Society for Metals, Materials Park, Ohio, 1990.
[17] D. Vanderbilt, Phys. Rev. B 41 (1990) 7892–7895.
[18] R. Agarwal, H. Feufel, F. Sommer, J. Alloy Compd. 217 (1995) 59–64.
[19] M. Giovannini, A. Saccone, R. Marazza, R. Ferro, Metall. Mater. Trans. A 26 (1) (1995) 5–10.
[20] L.Y. Wei, G.L. Dunlop, H. Westengen, Metall. Mater. Trans. A 26 (8) (1995) 1947–1955.
[21] L.Y. Wei, G.L. Dunlop, H. Westengen, Metall. Mater. Trans. A 26 (7) (1995) 1705–1716.
[22] C. Kittel, Introduction to Solid State Physics, 7th ed., Wiley, New York, 1996, p. 54, table I; the data in this revised table are supplied by L. Brewer (after LBL report 3720 Rev. 1977).
[23] D.E. Turner, Z.Z. Zhu, C.T. Chan, K.M. HO, Phys. Rev. B 55 (1997) 13842–13852.
[24] A. Delin, L. Fast, B. Johanssson, O. Eriksson, J.M. Wills, Phys. Rev. B 58 (1998) 4345–4351.
[25] W. Kraus, G. Nolze, Program PowderCell 2.4, FIMRT, Berlin, Germany, 2000.
[26] W. Wu, Y. Wang, X. Zheng, L.J. Chen, Z. Liu, J. Mater. Sci. Lett. 22 (6) (2003) 445–447.
[27] C. Guo, Z. Du, J. Alloy Compd. 385 (2004) 109–113.
[28] B. Belgacem, S. Yahyaoui, P. Yu Demchenko, et al., Acta Cryst. E61 (2005) i155–i157.
[29] A. Berche, Ph.D. Thesis, Aix Marseille University, 2007 (in French).
[30] Y.-F. Wang, W.-B. Zhang, Z.-Z. Wang, Comp. Mater. Sci. 41 (2007) 78–85.
[31] M. Pozzo, D. Alfe, Phys. Rev. B 77 (2008) 104103-1–104103-8.
[32] A. Berche, F. Marinelli, G. Mikaelian, J. Rogez, M.-C. Record, J. Alloys Compd. 475 (2009) 79–85.
[33] S. Baroni, A. Dal Corso, S. de Gironcoli, P. Giannozzi, C. Cavazzoni, G. Ballabio, S. Scandolo, G. Chiarotti, P. Focher, A. Pasquarello, K. Laasonen, A. Trave, R. Car, N. Marzari, A. Kokalj, http://www.pwscf.org/.